



Evaluation of electro-oxidation of biologically treated landfill leachate using response surface methodology

Hui Zhang*, Xiaoni Ran, Xiaogang Wu, Daobin Zhang

Department of Environmental Engineering, Wuhan University, P.O. Box C319, Luoyu Road 129#, Wuhan 430079, China

ARTICLE INFO

Article history:

Received 2 December 2010
Received in revised form 24 January 2011
Accepted 25 January 2011
Available online 1 February 2011

Keywords:

Landfill leachate
Electro-oxidation
Ammonia removal
COD removal
GC–MS
Box–Behnken method

ABSTRACT

Box–Behnken statistical experiment design and response surface methodology were used to investigate electrochemical oxidation of mature landfill leachate pretreated by sequencing batch reactor (SBR). Titanium coated with ruthenium dioxide (RuO₂) and iridium dioxide (IrO₂) was used as the anode in this study. The variables included current density, inter-electrode gap and reaction time. Response factors were ammonia nitrogen removal efficiency and COD removal efficiency. The response surface methodology models were derived based on the results. The predicted values calculated with the model equations were very close to the experimental values and the models were highly significant. The organic components before and after electrochemical oxidation were determined by GC–MS.

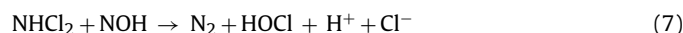
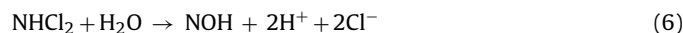
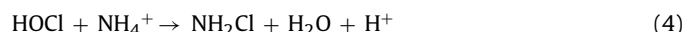
© 2011 Elsevier B.V. All rights reserved.

1. Introduction

In the past decades, there has been increased interest in the use of electrochemical oxidation for the treatment of landfill leachate [1–13]. During the electrolysis, the destruction of pollutants can be achieved via two different oxidation mechanisms: direct anodic oxidation, where the pollutants are destroyed at the anode surface, and indirect oxidation, where a mediator is electrochemically generated to carry out the oxidation [1,14]. It is believed that contaminants in the leachate are primarily destroyed via indirect oxidation by strong oxidants such as hypochlorite generated from anodic oxidation of chloride, which originally exists or is applied in the leachate [15]:



In this case, ammonia nitrogen in the leachate could be removed through the mechanism similar to “breakpoint reactions” [15]:



Hydroxyl radicals or other reactive species may also be generated and participate in the electrochemical oxidation of organics [8].

Although electrochemical methods have been successfully applied to the treatment of landfill leachate, it is fairly expensive compared with biological treatment. Therefore, electrochemical oxidation is not considered as a full treatment for landfill leachate but as a finishing stage in a combined process or as an auxiliary unit in emergency situations [16]. Cossu et al. used Ti/PbO₂ and Ti/SnO₂ anodes to remove chemical oxygen demand (COD) and ammonia nitrogen from landfill leachate after pretreated by aerobic lagooning, denitrification, and activated sludge processes [16]. Sayadi and co-authors employed integrated membrane bioreactor (MBR)-electrochemical process to remove COD, ammonia nitrogen and color from the stabilized landfill leachate [8,9]. Ortiz and co-authors used boron-doped diamond (BDD) electrodes to remove COD and ammonia nitrogen from biologically/physicochemically pretreated leachates in both laboratory scale and pilot plant scale [3–6,11,12]. In these investigations, the traditional one-factor-at-a-time approach was used to study the effects of various factors on COD, ammonia nitrogen or color removal. This method estimates the effect of a single variable on electrochemical process while keeping all other variables at a fixed condition. But this classical approach is a time consuming method for multivariable systems and it cannot estimate the interactions among the

* Corresponding author. Tel.: +86 27 68775837; fax: +86 27 68778893.
E-mail address: eeng@whu.edu.cn (H. Zhang).

Table 1
Average characterization of raw, biological pre-treated leachate.

| Parameter | Raw leachate | Biological effluent |
|--|--------------|---------------------|
| pH | 8.10 | 8.85 |
| NH ₄ ⁺ -N (mg/L) | 2470 | 520 |
| COD (mg/L) | 2400 | 560 |
| BOD ₅ (mg/L) | 370 | 50 |
| BOD ₅ /COD | 0.154 | 0.089 |
| Cl ⁻ (mg/L) | 2900 | 831 |
| Alkalinity (CaCO ₃ mg/L) | 10,500 | 1500 |

variables [17–21]. Response surface methodology (RSM), a multivariate technique which mathematically fits the experimental domain studied in the theoretical design through a response function [22], is then proposed to solve these problems [17–21]. The main types of RSM designs include three-level factorial design, central composite design (CCD), Box–Behnken design and D-optimal design [17–19,23]. As one of the RSM designs, Box–Behnken design is known as a modified central composite experimental design [17–19,23]. It is an independent, rotatable quadratic design with no embedded factorial or fractional factorial points in which the variable combinations are at the midpoints of the edges of the variable space and at the center [17–19,23]. A comparison between Box–Behnken design and other RSM designs has demonstrated that Box–Behnken design is slightly more efficient than CCD, but much more efficient than the three-level full factorial designs [19]. Moreover, it requires fewer experiments than other RSM designs with the same number of factors [17–19,23]. For example, only 15 runs are needed for a three-factor experimental design. However, there was little report on the electrochemical oxidation of raw leachate or biologically/physicochemically pretreated leachate using RSM or other statistical experiment design approach [10,13,24–26]. As a result, RSM with Box–Behnken design was used in this study to verify the various interactions of responsible factors for the objectives such as ammonia nitrogen removal and COD removal, as well as to investigate the effects of three variables on the objectives during the electrochemical oxidation of biologically treated leachate. The three variables investigated include current density, inter-electrode gap and reaction time. The organic components before and after electro-oxidation were also investigated by GC–MS.

2. Materials and methods

2.1. Landfill leachates sampling

Leachate samples were taken with polyethylene bottles from April 2009 to May 2009 from a landfill at Wuhan (China), which has been in operation since 2003. Samples taken were preserved in refrigerator at 4 °C in accordance with the Standard Methods [27]. The physicochemical characteristics of the raw leachate are shown in Table 1.

2.2. Sequencing batch reactor (SBR)

Biological pretreatment of raw leachate was carried out in a SBR with a working volume of 10 L. An air-compressor was used for aeration, and a mechanical stirrer with 150 rpm was used to provide the mixing of substrate and biomass in the reactor. Effluent and sludge were drawn by siphon, and the solid residence time was controlled at about 20 days. The SBR system was operated in the following sequential phases: 0-h feeding (3.5 L leachate was fed instantaneously), 8-h aeration, 3-h mechanical agitation, 6-h aeration, 5-h mechanical agitation, 1-h settling, and 0.25-h decant. Initially, the seeding sludge from a landfill

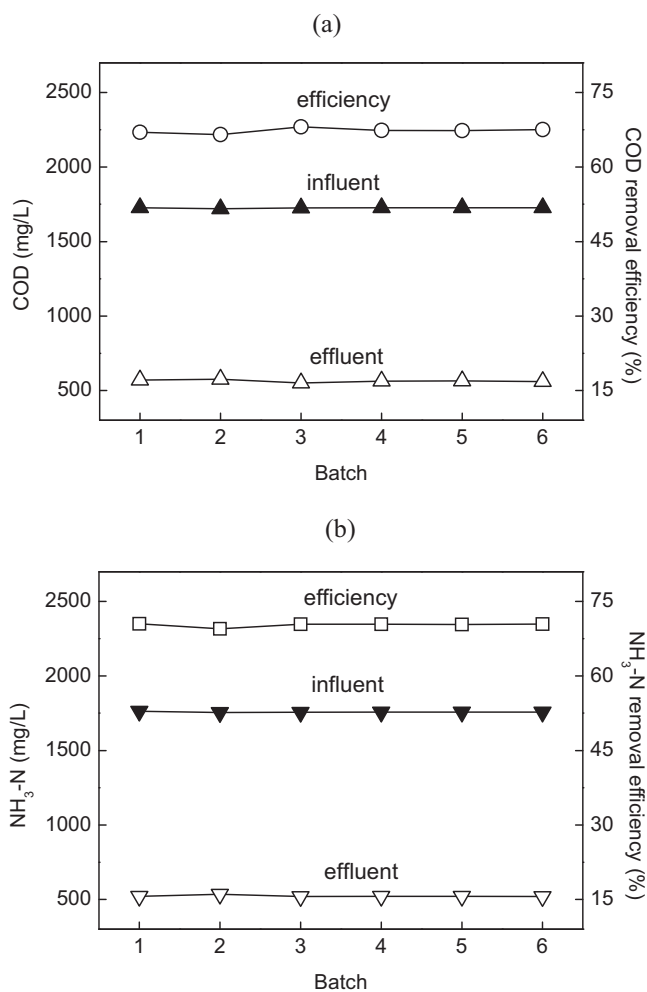


Fig. 1. The ammonia nitrogen (a) and COD (b) removal for various SBR treatment cycles.

leachate treatment plant was acclimatized to the landfill leachates. Organic loading was increased progressively till the influent COD reached 1720–1727 mg/L. Then the SBR system was operated for six cycles and the results are presented in Fig. 1. The mixed liquor suspended solids (MLSS) concentration was within the range of 3500–4000 mg/L during the experiments. The effluent from the SBR system was stored in a reservoir and its characteristics were analyzed (Table 1) before used in the electro-oxidation experiments.

2.3. Electrochemical reactor

The electrochemical oxidation experiments were conducted in a rectangular electrolytic cell which has been used in our previous studies [28–30]. The reactor containing 200 mL leachate was immersed in a water bath to maintain the temperature at 35 ± 2 °C. Electrolyses were operated under constant current conditions using a direct current (DC) power supply (Model WYK-305, Yangzhou Jintong Source Co., Ltd., China). A 5 cm × 11.9 cm plate anode (Ti/RuO₂–IrO₂) and a plate cathode (stainless steel) of the same dimensions were arranged parallel to each other and were dipped in the leachate. The working surface area of the electrode was 31.5 cm². A magnetic stirrer (Model 78-1, Hangzhou Instrument Motors Factory, China) provided mixing of the solution in the reactor.

2.4. Analytical methods

The solution pH was measured with a Mettler-Toledo FE20/EL20 pH meter. Alkalinity was determined using titration method according to the Standard Methods [27]. COD was determined using a closed reflux, colorimetric method based on Standard Methods [27]. Five-day biological oxygen demand (BOD₅) was measured by the respirometric method (WTW Oxitop®IS6, Germany). Ammonia nitrogen was analyzed using Nessler's reagent colorimetric method according to the National Standard of the People's Republic of China (GB 7479-87) [31]. Chloride was measured using argentometric method according to the Standard Methods [27].

The intermediate reaction products of reaction were identified by GC-MS (Shimadzu GCMS-QP2010 Plus, Japan). Samples for GC-MS analysis were prepared by following the procedure reported by Lei et al. [2]. A 50 mL leachate sample was initially extracted with CH₂Cl₂ (HPLC grade) under neutral condition, then in alkaline condition (pH 12) by adding drops of NaOH solution, and then in acidic condition (pH 2) by adding some 1/9 (in volume) H₂SO₄ using separating funnel. Each extraction was done twice with 10 mL of CH₂Cl₂. The combined extract (about 60 mL) was dehydrated by anhydrous Na₂SO₄ and concentrated to 0.4 mL at 43 °C by rotary evaporation before being used for GC-MS analyses. A HP-5MS capillary column (30 m length × 0.32 mm ID × 0.25 μm film thickness) was employed for GC separation. The GC equipment was operated in a temperature programmed mode with an initial temperature of 50 °C held for 2 min, then ramped to 300 °C with a 4 °C/min rate and held for 15 min. The injector and transfer-line temperature was 300 °C. The injector was in splitless mode with 1 μL injection volume. Helium was used as a carrier gas at a flow-rate of 5.5 mL/min. MS detected at voltage 1.05 kV, EI 70 eV, scan field 45–500 *m/z*, and ion source temperature 200 °C.

3. Experimental design

Box-Behnken statistical experiment design and the response surface methodology were employed to investigate the effects of the three independent variables on the response functions. The independent variables were current density (X_1), inter-electrode gap (X_2), and reaction time (X_3). The low, center and high levels of each variable are designated as -1, 0, and +1, respectively as illustrated in Table 2. The experimental levels for each variable were selected based on the literature values, available resources and results from preliminary experiments.

The dependent variables or objective functions were ammonia nitrogen removal efficiency (Y_1) and COD removal efficiency (Y_2). Box-Behnken design requires an experiment number according to $N = k^2 + k + c_p$, where (k) is the factor number and (c_p) is the repli-

Table 2

Experimental range and levels of the independent variables.

| Variables | Symbol | -1 | 0 | +1 |
|--|--------|-----|-----|-----|
| Current density (mA cm ⁻²) | X_1 | 26 | 47 | 68 |
| Inter-electrode gap (cm) | X_2 | 0.7 | 2.2 | 3.7 |
| Reaction time (min) | X_3 | 30 | 60 | 90 |

cate number of the central point [13,32,33]. The total number of experiments in this study was 15 based on 3 levels and a 3 factor experimental design, with three replicates at the center of the design for estimation of a pure error sum of squares. Experimental data from the Box-Behnken design could be analyzed and fitted to a second-order polynomial model using Design Expert software:

$$Y = \beta_0 + \sum_{i=1}^k \beta_i X_i + \sum_{i=1}^{j-1} \sum_{j=1}^k \beta_{ij} X_i X_j + \sum_{i=1}^k \beta_{ii} X_i^2 + e_i \quad (8)$$

where Y is the response for ammonia nitrogen removal (Y_1) or COD removal (Y_2), X_i and X_j are variables, β_0 is a constant coefficient, β_i is a coefficient that determines the influence of parameter i in the response (linear term), β_{ij} refers to the effect of the interaction among variables i and j , β_{ii} is a parameter that determines the shape of the curve (quadratic effect), k is the number of studied factors and e_i is the error [10]. The coded values of the process parameters in Eq. (8) could be determined by the following equation [13,34,35]:

$$X_i = \frac{x_i - x_0}{\Delta x_i} \quad (9)$$

where X_i is dimensionless coded value of the i th independent variable, x_i is the uncoded value of the i th independent variable, x_0 is the uncoded i th independent variable at the center point, and Δx_i is the step change value between low level (-1) and high level (+1).

4. Results and discussion

Table 3 illustrates the experimental results of ammonia nitrogen and COD removal efficiencies. Based on Table 3, the main effects plot and the interaction plots for ammonia nitrogen and COD removal efficiencies were developed as illustrated in Figs. 2 and 3.

Fig. 2 illustrates the effects of three factors on the response variable. This type of representation shows the contribution to the response factor of changing one of the variables selected for electrochemical process. As can be seen, the effects of all three factors on ammonia nitrogen removal efficiency are positive, i.e., the greater removal efficiency could be achieved at high level (+1) of each factor than that at low level (-1) of the factor. On the other hand, the effect of current density or reaction time on COD removal efficiency is positive, while that of inter-electrode gap is negative. This means

Table 3

Design matrix in coded units and the experimental responses.

| Standard order | Current density (X_1) | Inter-electrode gap (X_2) | Reaction time (X_3) | Ammonia removal efficiency (%) | COD removal efficiency (%) |
|----------------|---------------------------|-------------------------------|-------------------------|--------------------------------|----------------------------|
| 1 | -1 | -1 | 0 | 31.7 | 34.9 |
| 2 | 1 | -1 | 0 | 70.5 | 66.4 |
| 3 | -1 | 1 | 0 | 33.7 | 37.1 |
| 4 | 1 | 1 | 0 | 87.6 | 47.2 |
| 5 | -1 | 0 | -1 | 11.9 | 24.2 |
| 6 | 1 | 0 | -1 | 47.2 | 40.2 |
| 7 | -1 | 0 | 1 | 50.4 | 44.3 |
| 8 | 1 | 0 | 1 | 98.4 | 66.2 |
| 9 | 0 | -1 | -1 | 17.7 | 52 |
| 10 | 0 | 1 | -1 | 27.1 | 33.6 |
| 11 | 0 | -1 | 1 | 68.7 | 63.1 |
| 12 | 0 | 1 | 1 | 98.4 | 66.2 |
| 13 | 0 | 0 | 0 | 60 | 54 |
| 14 | 0 | 0 | 0 | 59.3 | 54 |
| 15 | 0 | 0 | 0 | 58.8 | 54.1 |

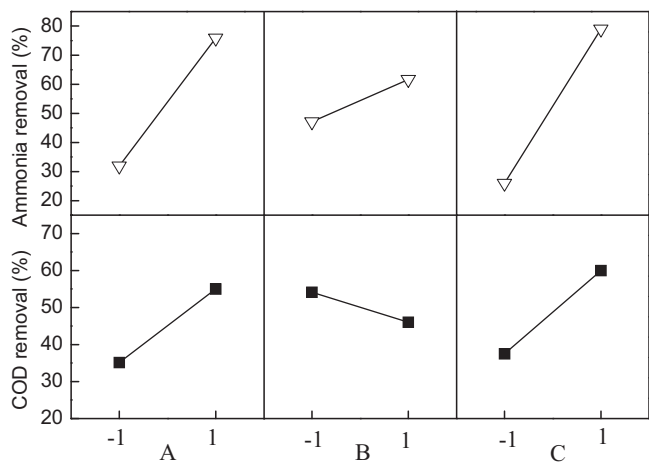


Fig. 2. Main effects plot for ammonia nitrogen and COD removal efficiencies (A—current density; B—inter-electrode gap; C—reaction time; (▽) ammonia; (■) COD).

that high level (+1) of current density or reaction time would lead to the greater COD removal, but the greater COD removal could be obtained at low level (−1) of inter-electrode gap. Since COD was removed mainly through the direct anodic oxidation or by electro-generated hydroxyl radicals, the smaller inter-electrode gap would favor direct oxidation and the diffusion of hydroxyl radicals electro-chemically generated at the anode. In Fig. 2, the slope of the plot is indicative of the importance of the variable on the response factor. It can be seen that the effect of inter-electrode gap on the response variable is much less important than that of current density and reaction time. It should be noted that Fig. 2 just depicts the main effects plot for ammonia nitrogen or COD removal efficiency. The dependence between the response variable (ammonia nitrogen or COD removal efficiency) and all the design variables was not necessarily as linearly as depicted in Fig. 2. This will be revealed from the quadratic RSM model.

Fig. 3 indicates interaction plots among the three factors. Generally, an interaction may occur if the change in the response factor from the low level to the high level of one independent variable differs from the change in the response factor at the same two levels of another independent variable [13,36,37]. In other words, the effect of one design variable is dependent upon the other design variable [36,38]. The interaction effects on ammonia nitrogen removal between current density and reaction time and that between inter-

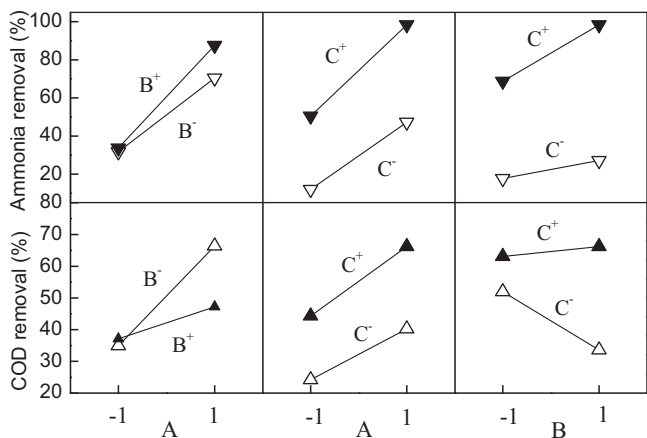


Fig. 3. Interaction plots for ammonia nitrogen and COD removal efficiencies (A—current density; B—inter-electrode gap; C—reaction time; (▽) ammonia; (▲) COD).

Table 4
ANOVA test for response function Y_1 (ammonia removal efficiency).

| Source | Degree of freedom | Dum of squares | Mean square | F ratio | Prob > F |
|-------------|-------------------|----------------|-------------|---------|----------|
| Model | 3 | 9913.40 | 3304.47 | 71.64 | <0.0001 |
| X_1 | 1 | 3872.00 | 3872.00 | 83.95 | <0.0001 |
| X_2 | 1 | 423.40 | 423.40 | 9.18 | 0.0115 |
| X_3 | 1 | 5618.00 | 5618.00 | 121.80 | <0.0001 |
| Residual | 11 | 507.37 | 46.12 | | |
| Lack of fit | 9 | 506.64 | 56.29 | 154.94 | 0.0064 |
| Pure error | 2 | 0.73 | 0.36 | | |
| Cor total | 14 | 10420.78 | | | |

electrode gap and reaction time are insignificant due to almost parallel plots as shown in Fig. 3 [36]. This was also confirmed by the high probability values ((Prob > F) > 0.1) through analysis of variance (ANOVA) [34,39–41]. Although the plot between current density and inter-electrode gap is crossed, the Fisher's F -test showed the value of Prob > F was 0.28, which was higher than 0.1. This indicates that the interaction between current density and inter-electrode gap is insignificant [34,39–41]. Therefore, all the interaction items (X_1X_2 , X_1X_3 and X_2X_3) would be dropped from the RSM model for ammonia removal.

Although the plot of the interaction effect on COD removal between current density and reaction time is almost parallel, the Fisher's F -test showed the value of Prob > F was 0.02, which was less than 0.05. This indicates that the interaction between current density and reaction time is significant [34]. Meanwhile, the plots of the interactions among other variables are crossed or tending to cross, indicating that the interaction effects are significant. This was verified by the low probability value ((Prob > F) < 0.05) through ANOVA analysis [34].

After all the insignificant factors were removed according to the confidence level selected ((Prob > F) > 0.1) [34,39–41], the ultimate RSM models were determined to calculate ammonia nitrogen removal efficiency and COD removal efficiency in terms of the coded factors:

$$Y_1 = 54.76 + 22X_1 + 7.27X_2 + 26.5X_3 \quad (10)$$

$$Y_2 = 54.03 + 9.94x_1 - 4.04x_2 + 11.23x_3 - 5.35x_1x_2 + 1.48x_1x_3 + 5.38x_2x_3 - 8.82x_1^2 + 1.18x_2^2 - 1.49x_3^2 \quad (11)$$

and in terms of actual factors:

$$Y_1 = -58.15 + 1.05x_1 + 4.85x_2 + 0.88x_3 \quad (12)$$

$$Y_2 = -27.51 + 2.58x_1 - 4.19x_2 + 0.20x_3 - 0.17x_1x_2 + 2.3E + 0.3x_1x_3 + 0.12x_2x_3 - 0.02x_1^2 + 0.52x_2^2 - 1.6E - 0.3x_3^2 \quad (13)$$

ANOVA results of the models presented in Tables 4 and 5 indicate that they can be used to navigate the design space. The model F -values of 71.64 and 490.31 in the tables imply that the models are significant for ammonia removal and COD removal, respectively. Adequate precision measures the signal to noise ratio and a ratio greater than 4 is desirable [40,42–44]. Therefore, in the models of ammonia removal and COD removal, the ratios of 27.66 and 69.28 indicate adequate signals for the models to be used to navigate the design space.

The normality of the data can be checked by constructing a normal probability plot of the residuals. The residuals are normally distributed if the points on the plot follow a straight line then [10,33,44]. Fig. 4 shows normal probability plot of residual values. It could be seen that the normality assumption was confirmed.

Table 5
ANOVA test for response function Y_2 (COD removal efficiency).

| Source | Degree of freedom | Dum of squares | Mean square | F ratio | Prob > F |
|-------------|-------------------|----------------|-------------|---------|----------|
| Model | 9 | 2470.43 | 274.49 | 490.31 | <0.0001 |
| X_1 | 1 | 790.03 | 790.03 | 1411.19 | <0.0001 |
| X_2 | 1 | 130.41 | 130.41 | 232.95 | <0.0001 |
| X_3 | 1 | 1008.00 | 1008.00 | 1800.54 | <0.0001 |
| X_1X_2 | 1 | 114.49 | 114.49 | 204.51 | <0.0001 |
| X_1X_3 | 1 | 8.7 | 8.7 | 15.54 | 0.0109 |
| X_2X_3 | 1 | 115.56 | 115.56 | 206.42 | <0.0001 |
| X_1^2 | 1 | 287.02 | 287.02 | 512.68 | <0.0001 |
| X_2^2 | 1 | 5.17 | 5.17 | 9.24 | 0.0288 |
| X_3^2 | 1 | 8.22 | 8.22 | 14.68 | 0.0122 |
| Residual | 5 | 2.8 | 0.56 | | |
| Lack of fit | 3 | 2.79 | 0.93 | 279.25 | 0.0036 |
| Pure error | 2 | 6.667E-003 | 3.333E-003 | | |
| Cor total | 14 | 2473.23 | | | |

The goodness of fit of the models was checked by the determination coefficient (R^2). The closer the R^2 values are to 1, the stronger the models are and the better they predicts ammonia removal and COD removal, respectively. The values of the determination coefficient ($R^2 = 0.951$ for ammonia nitrogen removal and

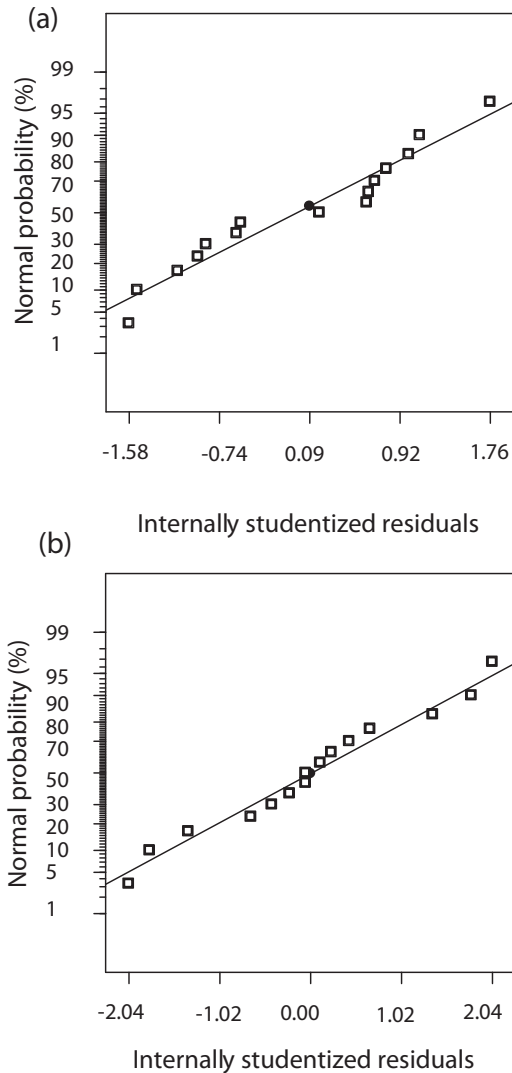


Fig. 4. Normal probability plot of the internally studentized residuals for the: (a) ammonia removal and (b) COD removal.

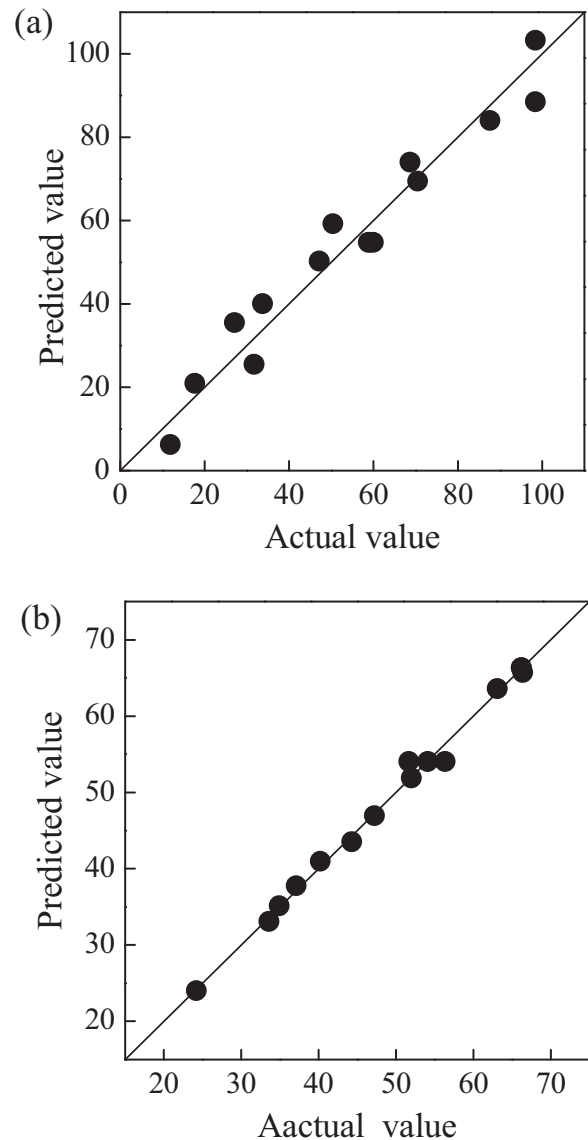


Fig. 5. Predicted versus actual values plot for (a) ammonia removal and (b) COD removal.

$R^2 = 0.999$ for COD removal) indicate that only 4.87% (ammonia nitrogen removal) and 0.11% (COD removal) of the variability in the response were not explained by the models. In addition, the values of adjusted determination coefficient ($R^2_{adj} = 0.938$ for ammonia nitrogen removal and $R^2 = 0.997$ for COD removal) were also very high, showing a high significance of the models. The adjusted determination coefficient corrects the determination coefficient for the sample size and the number of terms in the model. If there are many terms in the model and the sample size is not very large, the R^2_{adj} value may be noticeably smaller than the R^2 value [45]. In this study, the R^2_{adj} value was very close to the R^2 value, which is similar to the reports by Liu et al. [45] and Yetilmezsoy et al. [35]. In addition, the values of predicted R^2 are also high to support for a high significance of the models. The predicted R^2 of 0.902 for ammonia nitrogen removal and 0.982 for COD removal are in reasonable agreement with the adjusted R^2 of 0.938 for ammonia nitrogen removal and 0.997 for COD removal, respectively. The statistical significance of the model was further evident from the fact that the values calculated with the predictive equations were very close to the experimental values (Fig. 5).

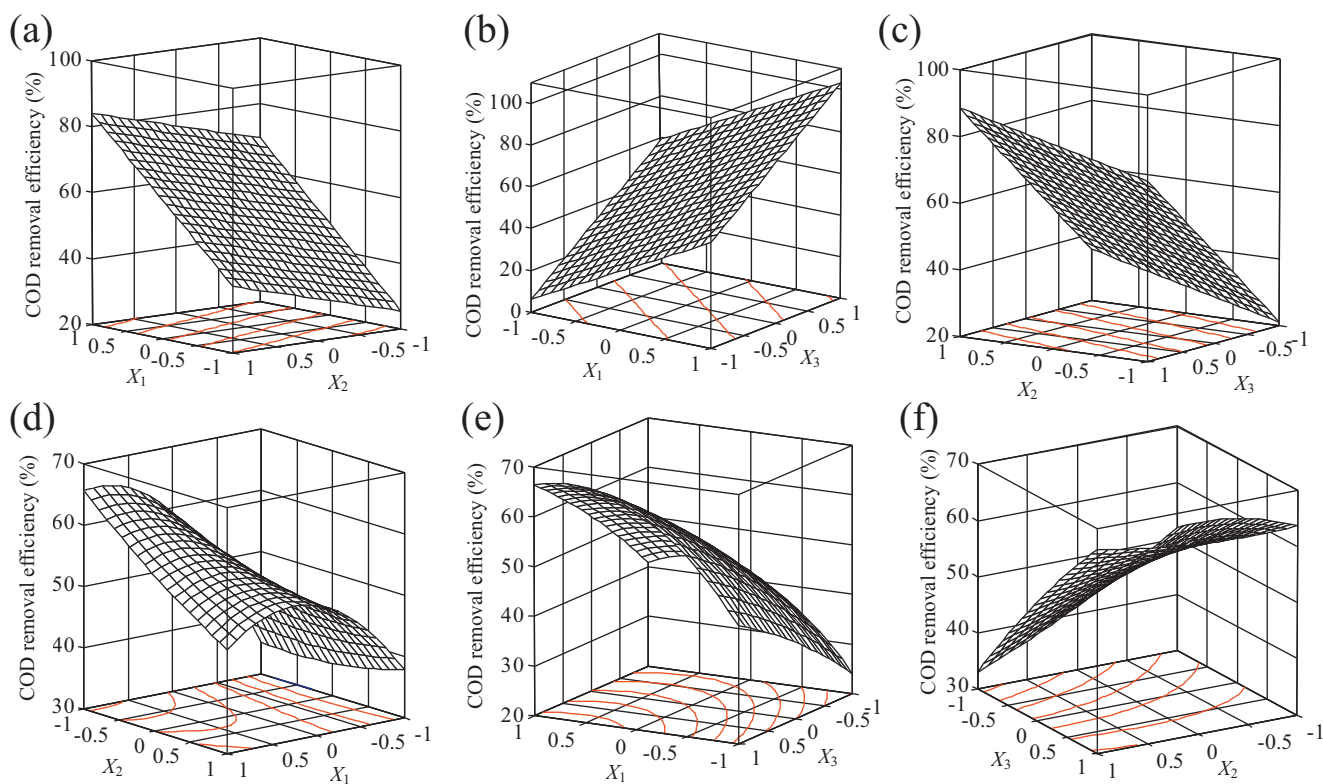


Fig. 6. Response surface plots of percent ammonia (a–c) and COD (d–f) removals.

This illustrated that the prediction of experimental data is quite satisfactory.

The response surface plots were developed based on the RSM equations (10) and (11), which were represented as a function of two factors at a time, holding other factors at a fixed level (center level). As can be seen in Fig. 5, ammonia nitrogen removal efficiencies were much higher than COD removal efficiencies during the electrolysis. This is in agreement with the reports by Feki et al. [8] when biological treated effluent of leachate was oxidized electrochemically using different anode materials such as platinized titanium grid, PbO_2 and graphite plates, and also by Chiang et al. [24] and Zhang et al. [13] when raw leachate was treated in a two-dimensional and three-dimensional electrode reactor respectively. During the electrochemical oxidation of landfill leachate, both ammonia nitrogen and COD would be removed simultaneously and there would be a competition between ammonia nitrogen removal and COD removal. According to the report by Deng and Englehardt [1], the rule of competition between removal of ammonia nitrogen and COD seems to be that the removal of ammonia nitrogen is greater than that of COD when indirect oxidation is prevalent, whereas COD removal takes priority under direct anodic oxidation. The greater ammonia nitrogen removal than COD removal indicated that indirect oxidation is dominant during electrochemical reaction [8] (Fig. 6).

Fig. 4(a)–(c) shows that ammonia removal increases with current density, inter-electrode gap and reaction time. However, the dependence of COD removal on current density or inter-electrode gap was different from that of ammonia removal. COD removal efficiency increased with the increasing current density, but further increase of current density would lead to the decrease of COD removal efficiency (Fig. 4(d) and (e)). This is similar to our previous study when raw leachate was oxidized in a three-dimensional electrochemical reactor [13]. At lower current densities, direct

anodic oxidation of COD is favored against chlorine evolution at the anode [6]. Hence the increase in current density would lead to the increase of COD removal. But further increase of current density would enhance chlorine generation [7], and hence the direct anodic oxidation of COD would be depressed. In the meantime, the removal of ammonia nitrogen would be dominant in the competition between ammonia nitrogen removal and COD removal by the indirect oxidation [24]. Consequently, COD removal efficiency would decrease with current density after the highest COD removal was achieved. Contrary to the ammonia removal, COD removal decreased with inter-electrode gap. This is due to the different oxidation mechanisms of ammonia and COD, i.e., the removal of ammonia is favored when indirect oxidation is dominant, whereas COD removal takes priority under direct anodic oxidation [3].

In order to gain insight into the organics in the leachate before and after electro-oxidation, leachate contents in the influent and effluent of the electrochemical reactor were analyzed by GC–MS. The chromatogram shown in Fig. 7 reveals the presence of at least 50 types of organic components in the influent whose match percent was not less than 80%, including 15 alkanes and olefins, 7 alcohols, 3 aldehyde and ketones, 3 amides and nitrile, 1 aromatic hydrocarbon, 7 carboxylic acids, 10 esters, 2 heterocyclic compounds and 2 hydroxybenzenes. Some of the compounds, such as phthalates, are known as priority pollutants defined by US EPA [46], which were also observed in other leachate by Benfenati et al. [47], Öman and Junestedt [48], and Trzcinski and Stuckey [49,50]. After electrochemical oxidation, about 20 organic pollutants were not detected. However, some new compounds were detected in the effluent of the electrochemical reactor. This is due to the effluent from SBR mainly contained non-biodegradable dissolved organic matter (DOM) such as humic acids and fulvic acids which were hard to be detected by GC–MS [2,51]. After electro-oxidation, DOM

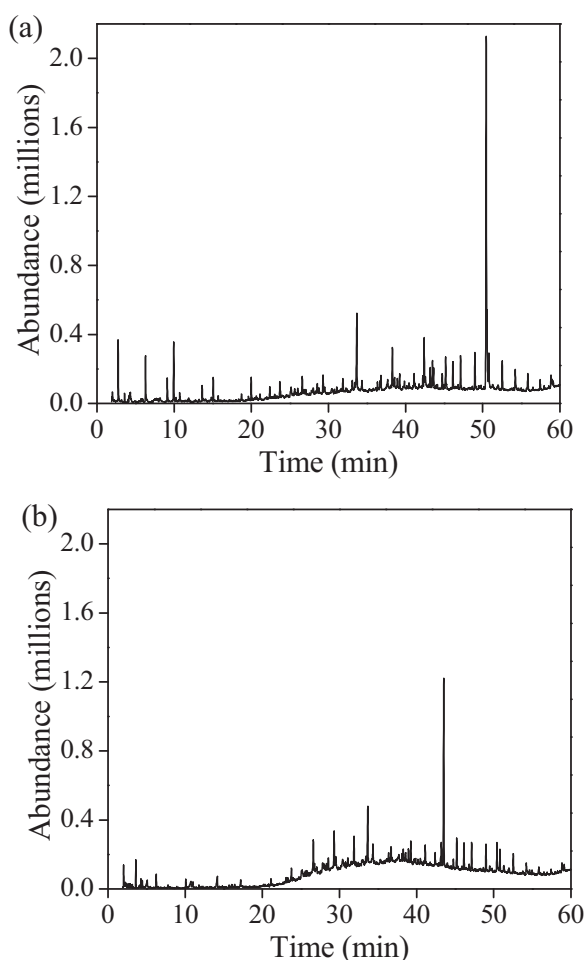


Fig. 7. Chromatogram for organics in the influent (a) and effluent (b) of the electrochemical reactor.

would be oxidized to small organic compounds, which were more readily detected by GC–MS.

5. Conclusions

Box–Behnken statistical experiment design was proven to be a suitable response surface methodology to determine the effects of operative variables (current density, inter-electrode gap and reaction time) and their interactions on the electro-oxidation of biologically treated landfill leachate. The analysis of variance (ANOVA) indicated neither the interaction effect nor the quadratic effect was significant on ammonia nitrogen removal, while both effects were significant on COD removal. The response surface methodology models were derived after the insignificant terms were excluded. The models were significant and could fit the experimental data well. About 50 pollutants were detected in the leachate by GC–MS, of which 20 organics were completely removed after electrochemical oxidation.

Acknowledgements

This study was supported by SRF for ROCS, SEM, China (Grant No. [2001]498), China Hubei Provincial Science and Technology Department through “The Gongguan Project” (Grant No. 2003AA307B01), Wuhan Science and Technology Bureau through “The Gongguan Project”, China (Grant No. 201060723313) and the National High-Tech R&D Program (863 Program) of China (Grant

No. 2008AA06Z332). We appreciate the valuable comments of the anonymous reviewers.

References

- [1] Y. Deng, J.D. Englehardt, Electrochemical oxidation for landfill leachate treatment, *Waste Manage.* 27 (2007) 380–388.
- [2] Y.M. Lei, Z.M. Shen, R.H. Huang, W.H. Wang, Treatment of landfill leachate by combined aged-refuse bioreactor and electro-oxidation, *Water Res.* 41 (2007) 2417–2426.
- [3] A. Cabeza, A.M. Urriaga, I. Ortiz, Electrochemical treatment of landfill leachates using a boron-doped diamond anode, *Ind. Eng. Chem. Res.* 46 (2007) 1439–1446.
- [4] A. Cabeza, A. Urriaga, M.-J. Rivero, I. Ortiz, Ammonium removal from landfill leachate by anodic oxidation, *J. Hazard. Mater.* 144 (2007) 715–719.
- [5] A. Urriaga, A. Rueda, A. Anglada, I. Ortiz, Integrated treatment of landfill leachates including electrooxidation at pilot plant scale, *J. Hazard. Mater.* 166 (2007) 1530–1543.
- [6] A. Anglada, A. Urriaga, I. Ortiz, Pilot scale performance of the electro-oxidation of landfill leachate at boron-doped diamond anodes, *Environ. Sci. Technol.* 43 (2009) 2035–2040.
- [7] N.N. Rao, M. Rohit, G. Nitin, P.N. Parameswaran, J.K. Astik, Kinetics of electrooxidation of landfill leachate in a three-dimensional carbon bed electrochemical reactor, *Chemosphere* 76 (2009) 1206–1212.
- [8] F. Feki, F. Aloui, M. Feki, S. Sayadi, Electrochemical oxidation post-treatment of landfill leachates treated with membrane bioreactor, *Chemosphere* 75 (2009) 256–260.
- [9] F. Aloui, F. Feki, S. Loukil, S. Sayadi, Application of combined membrane biological reactor and electro-oxidation processes for the treatment of landfill leachates, *Water Sci. Technol.* 60 (2009) 605–614.
- [10] M.J.K. Bashir, M.H. Isa, S.R.M. Kuttu, H.A. Zarizi Bin Awang, S. Aziz, I.H. Mohajeri, Farooqi, Landfill leachate treatment by electrochemical oxidation, *Waste Manage.* 29 (2009) 2534–2541.
- [11] A. Anglada, A.M. Urriaga, I. Ortiz, Laboratory and pilot plant scale study on the electrochemical oxidation of landfill leachate, *J. Hazard. Mater.* 181 (2010) 729–735.
- [12] A. Anglada, D. Ortiz, A.M. Urriaga, I. Ortiz, Electrochemical oxidation of landfill leachates at pilot scale: evaluation of energy needs, *Water Sci. Technol.* 61 (2010) 2211–2217.
- [13] H. Zhang, Y.L. Li, X.G. Wu, Y.J. Zhang, D.B. Zhang, Application of response surface methodology to the treatment landfill leachate in a three-dimensional electrochemical reactor, *Waste Manage.* 30 (2010) 2096–2102.
- [14] A. Anglada, A. Urriaga, I. Ortiz, Contributions of electrochemical oxidation to waste-water treatment: fundamentals and review of applications, *J. Chem. Technol. Biotechnol.* 84 (2009) 1747–1755.
- [15] L.C. Chiang, J.E. Chang, T.C. Wen, Electrochemical treatability of refractory pollutants in landfill leachate, *Hazard. Waste Hazard. Mater.* 12 (1995) 71–82.
- [16] R. Cossu, A.M. Polcaro, M.C. Lavagnolo, M. Mascia, S. Palmas, F. Renoldi, Electrochemical treatment of landfill leachate: oxidation at Ti/PbO₂ and Ti/SnO₂ anodes, *Environ. Sci. Technol.* 32 (1998) 3570–3573.
- [17] E.C. Catalkaya, F. Kargi, Effects of operating parameters on advanced oxidation of diuron by the Fenton's reagent: a statistical design approach, *Chemosphere* 69 (2007) 485–492.
- [18] E.C. Catalkaya, F. Kargi, Advanced oxidation of diuron by photo-Fenton treatment as a function of operating parameters, *J. Environ. Eng. ASCE* 134 (2008) 1006–1013.
- [19] F. Ay, E.C. Catalkaya, F. Kargi, A statistical experiment design approach for advanced oxidation of Direct Red azo-dye by photo-Fenton treatment, *J. Hazard. Mater.* 162 (2009) 230–236.
- [20] H. Zhang, H.J. Choi, P. Canazoc, C.-P. Huang, Multivariate approach to the Fenton process for the treatment of landfill leachate, *J. Hazard. Mater.* 161 (2009) 1306–1312.
- [21] M.A. Islam, V. Sakkas, T.A. Albanis, Application of statistical design of experiment with desirability function for the removal of organophosphorus pesticide from aqueous solution by low-cost material, *J. Hazard. Mater.* 170 (2009) 230–238.
- [22] A.P.M. Tavares, R.O. Cristovao, J.M. Loureiro, R.A.R. Boaventura, E.A. Macedo, Application of statistical experimental methodology to optimize reactive dye decolourization by commercial laccase, *J. Hazard. Mater.* 162 (2009) 1255–1260.
- [23] E.C. Catalkaya, F. Kargi, Advanced oxidation and mineralization of simazine using Fenton's reagent, *J. Hazard. Mater.* 168 (2009) 688–694.
- [24] L.C. Chiang, J.E. Chang, T.C. Wen, Indirect oxidation effect in electrochemical oxidation treatment of landfill leachate, *Water Res.* 29 (1995) 671–678.
- [25] A.G. Vlyssides, P.K. Karlis, G. Mahnken, Influence of various parameters on the electrochemical treatment of landfill leachates, *J. Appl. Electrochem.* 33 (2003) 155–159.
- [26] S. Mohajeri, H.A. Aziz, M.H. Isa, M.A. Zahed, M.J.K. Bashir, M.N. Adlan, Application of the central composite design for condition optimization for semi-aerobic landfill leachate treatment using electrochemical oxidation, *Water Sci. Technol.* 61 (2010) 1257–1266.
- [27] APHA, AWWA, WPCF, Standard Methods for the Examination of Water and Wastewater, 20th ed., American Public Health Association, American Water Works Association, Water Pollution Control Federation, Washington, DC, USA, 1998.

- [28] H. Zhang, D.B. Zhang, J.Y. Zhou, Removal of COD from landfill leachate by electro-Fenton method, *J. Hazard. Mater.* 135 (2006) 106–111.
- [29] H. Zhang, F. Liu, X.G. Wu, J.H. Zhang, D.B. Zhang, Degradation of tetracycline in aqueous medium by electrochemical method, *Asia Pac. J. Chem. Eng.* 4 (2009) 568–573.
- [30] H. Zhang, J. Wu, Z.Q. Wang, D.B. Zhang, Electrochemical oxidation of Crystal Violet in the presence of hydrogen peroxide, *J. Chem. Technol. Biotechnol.* 85 (2010) 1436–1444.
- [31] National Standard of the People's Republic of China, Water quality – Determination of ammonium – Nessler's reagent colorimetric method, GB 7479–87.
- [32] B.K. Tiwari, K. Muthukumarappan, C.P. O'Donnell, P.J. Cullen, Modelling colour degradation of orange juice by ozone treatment using response surface methodology, *J. Food Eng.* 88 (2008) 553–560.
- [33] K. Tarangini, A. Kumar, G.R. Satpathy, V.K. Sangal, Statistical optimization of process parameters for Cr(VI) biosorption onto mixed cultures of *Pseudomonas aeruginosa* and *Bacillus subtilis*, *Clean-Soil Air Water* 37 (2009) 319–327.
- [34] M. Rajasimman, R. Sangeetha, P. Karthik, Statistical optimization of process parameters for the extraction of chromium(VI) from pharmaceutical wastewater by emulsion liquid membrane, *Chem. Eng. J.* 150 (2009) 275–279.
- [35] K. Yetilmezsoy, S. Demirel, R.J. Vanderbei, Response surface modeling of Pb(II) removal from aqueous solution by *Pistacia vera* L.: Box–Behnken experimental design, *J. Hazard. Mater.* 171 (2009) 551–562.
- [36] M.P. Ormad, R. Mosteo, C. Ibarz, J.L. Ovelleiro, Multivariate approach to the photo-Fenton process applied to the degradation of winery wastewaters, *Appl. Catal. B: Environ.* 66 (2006) 58–63.
- [37] H. Zhang, Y.L. Li, X. Zhong, X.N. Ran, Application of experimental design methodology to the decolorization of Orange II using low iron concentration of photoelectro-Fenton process, *Water Sci. Technol.*, in press.
- [38] M. Sleiman, D. Vildoza, C. Ferronato, J.M. Chovelon, Photocatalytic degradation of azo dye Metanil Yellow: optimization and kinetic modeling using a chemometric approach, *Appl. Catal. B: Environ.* 77 (2007) 1–11.
- [39] G. Guven, A. Perendeci, A. Tanyolac, Electrochemical treatment of deproteinated whey wastewater and optimization of treatment conditions with response surface methodology, *J. Hazard. Mater.* 157 (2008) 69–78.
- [40] B.K. Korbahti, M.A. Rauf, Response surface methodology (RSM) analysis of photoinduced decoloration of toluidine blue, *Chem. Eng. J.* 136 (2008) 25–30.
- [41] I. Arslan-Alaton, G. Tureli, T. Olmez-Hanci, Treatment of azo dye production wastewaters using photo-Fenton-like advanced oxidation processes: optimization by response surface methodology, *J. Photochem. Photobiol. A: Chem.* 202 (2009) 142–153.
- [42] S. Ghafari, H.A. Aziz, M.H. Isa, A.A. Zinatizadeh, Application of response surface methodology (RSM) to optimize coagulation–flocculation treatment of leachate using poly-aluminum chloride (PAC) and alum, *J. Hazard. Mater.* 163 (2009) 650–656.
- [43] Y.H. Gong, H. Zhang, Y.L. Li, L.J. Xiang, S. Royer, S. Valange, J. Barrault, Evaluation of heterogeneous photo-Fenton oxidation of Orange II using response surface methodology, *Water Sci. Technol.* 62 (2010) 1320–1326.
- [44] S. Mohajeri, H.A. Aziza, M.H. Isa, M.A. Zahed, M.N. Adlan, Statistical optimization of process parameters for landfill leachate treatment using electro-Fenton technique, *J. Hazard. Mater.* 176 (2010) 749–758.
- [45] H.-L. Liu, Y.-W. Lan, Y.-C. Cheng, Optimal production of sulphuric acid by *Thiobacillus thiooxidans* using response surface methodology, *Process Biochem.* 39 (2004) 1953–1961.
- [46] L.H. Keith, W.A. Telliard, ES&T special report: priority pollutants. I. A perspective view, *Environ. Sci. Technol.* 13 (1979) 416–423.
- [47] E. Benfenati, G. Facchini, P. Pierucci, R. Fanelli, Identification of organic contaminants in leachates from industrial waste landfills, *Trac-Trend. Anal. Chem.* 15 (1996) 305–310.
- [48] C.B. Öman, C. Junstedt, Chemical characterization of landfill leachates—400 parameters and compounds, *Waste Manage.* 28 (2008) 1876–1891.
- [49] A.P. Trzcinski, D.C. Stuckey, Continuous treatment of the organic fraction of municipal solid waste in an anaerobic two-stage membrane process with liquid recycle, *Water Res.* 43 (2009) 2449–2462.
- [50] A.P. Trzcinski, D.C. Stuckey, Treatment of municipal solid waste leachate using a submerged anaerobic membrane bioreactor at mesophilic and psychrophilic temperatures: analysis of recalcitrants in the permeate using GC–MS, *Water Res.* 44 (2010) 671–680.
- [51] P.J. He, J.F. Xue, L.M. Shao, G.J. Li, D.J. Lee, Dissolved organic matter (DOM) in recycled leachate of bioreactor landfill, *Water Res.* 40 (2006) 1465–1473.